1

Introductory Concepts and Noise Fundamentals

Noise Issues in Optical Communications

With the first experiments in optical communications using tiny silica-glass optical fibers, more than 35 years ago, researchers pointed out the relevance of new, emerging, optical-based noise phenomena, unknown in contemporary electrical communications. Laser physics and early compound semiconductor technology were brought together at the start of the 1960s to create one of the most interesting devices of the twentieth century, namely the GaAs semiconductor laser, first demonstrated by Hall and Nathan in 1962. The invention of silica optical fiber at Corning Glass by C. Kao in 1970 led to the first experimental demonstration of digital optical transmission over a distance of a few hundred meters in early 1973 at AT&T Bell Labs, using an 870 nm GaAs laser source and a silicon PIN diode. That was the 'official' beginning of what today are optical fiber communications. During these 35 years, the amount of theoretical knowledge and technological progress in the optical fiber communication field has been enormous. Among the major improvements, knowledge and managing of optical noise impairments have greatly served to consolidate the success and the deployment of optical fiber communications.

1.1 Introduction: The Noise Concept

All physical systems are affected by noise. Noise degrades message intelligibility in all communication systems, including between people, leading to misunderstandings not dissimilar to those during noisy business meetings.

Why Does Noise Exist?

It would be more correct to pose the question in a slightly different way.

Noise and Signal Interference in Optical Fiber Transmission Systems Stefano Bottacchi

What is Noise?

After answering this question, we can better address the first question:

> *Noise is the effect of a very large number of single events, individually unpredictable and degrading the message recognition of the communication system we are using.*

We need both conditions mentioned above to set up a noisy phenomenon. In fact, dealing with only a small number of unpredictable events would allow individual random trajectories to be followed, tracing single-event statistics. On the other hand, if we were faced with a very large number of coherent and deterministic events, all of them behaving the same way and following the same phase trajectories, we would be able to collect them all, describing the whole flux of events in exactly the same way as a single deterministic event. Accordingly, the only task we need solve would consist in considering the amplified effect of the individual deterministic event.

> *The simultaneous presence of a very large number of unpredictable events leads unavoidably to the concept of noise.*

Under these conditions, we would no longer be able to extract the individual behavior and would instead sense only the population behavior, computing the expectation values, the mean, and the fluctuation. However, in order to identify a specific noise population and not an agglomerate of noisy populations, we require the homogeneous statistical behavior of the whole population. From a conceptual point of view, we need each individual component of the population to belong to the same space of phases affected by the same random behavior. Even if unpredictable, the behavior of each individual element of a single population must have common characteristics with all other population components in order to satisfy the same mathematical picture. As we will see in more detail later in this book, noise is fundamental in understanding the signal recognition process of *every* communication system, regardless of the transmission technique and the modulation format. According to the mathematical representation, *noise is a stochastic process* and we will indicate it with the generic notation $\underline{n}(t)$. *In this book we will use an underline to refer to random variables or stochastic processes.*

Noise is not a peculiarity of either electrical or optical communication systems or both. Noise in human communications manifests itself in many different forms: undesired signals, crosstalk, interference, misunderstandings, etc. Sometimes a person perceives noise as an unexpected and hence unrecognizable communication. Sometimes noise is the result of the chaotic evolution of myriads of entities. Noise is wasted energy. Heat is wasted work, according to the second law of thermodynamics. This book is simply an introduction to noise in optical communications and does not aim to delve into natural philosophy. So we will stop there. Noise is everywhere. It is part of our life.

1.2 Functional Classification of Noise

The most relevant parameter involved in the signal recognition process in every electrical or optical communication system using either analog or digital transmission techniques is the *Signal-to-Noise Ratio (SNR)*. The greater the SNR, the better the signal recognition process will be, leading to higher detection sensitivity. One fundamental question related to these

concepts is the minimum energy-per-bit of information (i.e. the signal) used by the communication system in order to satisfy the required performance. At first glance, it should be intuitive that increasing the noise power distributed in the bit interval should correspond to an increased amount of signal power in order to restore the required signal intelligibility. This reasoning would lead to the correct approach if the only noise terms were additive to the signal power. In this case, in fact, at increasing noise power, an equal increment of signal power would restore the original SNR and accordingly the original communication system performance. Unfortunately, in optical communication this is not the case. Except for a few noise components, all other contributions have either a linear or a quadratic dependence on the signal power level, leading to saturated behavior of the SNR and to limited and unimprovable performance of the optical communication system.

In the following section we will refer to either electrical or optical noise, introducing the functional classification of noise by means of relevant and quite common noise terms present in optical communication systems. We will represent the average (ensemble) power of the zero mean random process $\underline{n}(t)$ using the standard notation $\sigma^2_{\underline{n}}(t)$. If the random process satisfies the *ergodic* requirement, the ensemble average power is constant and the process becomes stationary. In Chapter 3 we will review in detail the fundamental concepts of the theory of stochastic processes, with particular attention to noise modeling.

1.2.1 Constant Term: Thermal Noise

Thermal noise is due to the thermal agitation of electric charges within a conductive medium and is governed by the Gaussian statistic on large-scale behavior. Individual electron trajectories are not predictable in any deterministic way owing to the large number of collisions per unit time they suffer along the random path and at every temperature above absolute zero (0 K). The random motion of free particles subjected to small acceleration terms compared with friction terms is described mathematically by the Wiener process $\underline{w}(t)$. The Wiener process [1] is the limiting form of the random-walk $\underline{x}_n(n\tau)$ for an indefinitely large number of events n and an indefinitely small time interval τ between any two successive collisions. With a very large collision density, the position variable $\underline{w}(t)$ tends to be distributed as a *Gaussian* function and the collision force $\underline{F}(t) = c_f\,\underline{w}'(t)$ assumes the *constant Power Spectral Density (PSD)*, leading to the fundamental concept of *White Gaussian Noise (WGN)*.

As already mentioned, Chapter 3 will be devoted entirely to reviewing the basic theory of stochastic processes, with particular attention to the general concepts used in modeling the different noise contributions encountered in optical fiber communication systems. Among the fundamental concepts regarding noise theory, the white noise model has a particular relevance. It refers to the stationary random process $\underline{x}(t)$ which is completely uncorrelated. From the mathematical point of view, the autocorrelation function $R_{\underline{x}}(\tau) = E\{\underline{x}(t+\tau)\underline{x}^*(t)\}$ of the white noise process $\underline{x}(t)$ coincides with the impulsive function $R_{\underline{x}}(\tau) = \delta(\tau)$, meaning that every two indefinitely close events $\underline{x}(t)$ and $\underline{x}(t+\tau)$, $\tau \to 0$, are still unpredictable.

The corresponding frequency representation of the impulsive autocorrelations leads to a constant spectrum power density, from which stems the term *white* noise. Of course, the indefinitely flat power spectrum of the white noise process is a very useful mathematical abstraction, but it leads to an infinite energy paradox. The white noise process assumes physical meaning after it is integrated within a finite time window. In conclusion, referring to electrical voltages or currents within the bandwidth capabilities of either electrical or optical

communication systems, the input equivalent *thermal noise* can be mathematically modeled as the *zero mean white Gaussian noise* random process characterized by the Gaussian *Probability Density Function (PDF)* and flat power spectral density.

One important property of thermal noise is that it is *independent of the signal level available at the same section*. We underline this property, specifying that *thermal noise is additive to the signal*. If we denote by $\underline{s}(t)$ and $\underline{n}(t)$ respectively the (random) signal and the additive thermal noise evaluated at the same section of the communication system, the total process $\underline{x}(t)$ is given by summing both quantities:

$$\underline{x}(t) = \underline{s}(t) + \underline{n}(t) \tag{1.1}$$

Increase in the value of the signal power brings with it a corresponding increment in the signal-to-noise power ratio. This suggests that the way to balance the thermal noise increment is to increase the signal power level by the same amount. However, even if the original system performance can be restored by operating in this way, the detection sensitivity of the system will be degraded (minimum detectable power penalty) by the same amount the noise power has increased. According to the above-mentioned notation, the average power of stationary thermal noise is represented by the term σ^2_{therm}.

1.2.2 Linear Term: Shot Noise

The second important example of noise functional dependence is represented by the *shot noise*. As clearly stated by the terminology used, this fundamental random process is a consequence of the granularity of the events that are detected. The shot noise is intimately related to the Poisson process and is not a peculiarity of electrical or optical communication systems. We can find examples of shot noise every time we are interested in counting events occurring at random times. Referring to electrical or optical quantities, both electrons and photons are particles that can be detected according to their arrival time $\underline{t}_i$. We will consider a constant flux μ_{p} of particles incident on the detector, and form the Poisson probability $P\{k_a \text{ in } t_a\}$ distribution of detecting k_a particles in a fixed time window t_a:

$$P\{k_a \text{ in } t_a\} = \frac{(\mu_{\text{p}} t_a)^k}{k!} \mathrm{e}^{-\mu_{\text{p}} t_a} \tag{1.2}$$

In addition, we will assume that any two nonoverlapping time intervals t_a and t_b, $t_a \cap t_b = \varnothing$, lead to independent measurements:

$$P\{k_a \text{ in } t_a, k_b \text{ in } t_b\} = P\{k_a \text{ in } t_a\} P\{k_b \text{ in } t_b\} \tag{1.3}$$

If the detection process satisfies both conditions above, the outcomes [1] will be called *random Poisson points*. The generation of shot noise in physical problems can be represented as a series of impulse functions $\delta(t - \underline{t}_i)$ localized at the random Poisson points $\underline{t}_i$:

$$\underline{x}(t) = \sum_i \delta(t - \underline{t}_i) \tag{1.4}$$

Although the impulsive function identifies the ideal detection of the particle (electron, photon), every measuring instrument must have a finite impulse response $h(t)$. We can easily

imagine the impulse sequence $\underline{x}(t)$ being applied at the input of detection mechanisms whose output accordingly shows the following form:

$$\underline{s}(t) = \sum_i h(t - \underline{t}_i) \tag{1.5}$$

The random process $\underline{s}(t)$ is known as *shot noise*. The electrical quantity $\underline{s}(t)$ associated with the detection mechanism, either voltage or current, will be distributed according to the Poisson distribution (1.2) and to the system impulse response $h(t)$. The derivation of the probability density function of the shot noise represents an interesting case of mathematical modeling of a noise process, and it will be discussed in detail in Chapter 2. The probability density function of shot noise is not Gaussian and, in particular for *low-density shot noise processes*, as in the case of the electron or photon counting process, it depends strongly on the system impulse response $h(t)$. We will address these concepts properly later on. For the moment, it is important to remark only that the *high-density shot noise process* is fairly well approximated by Gaussian statistics, irrespective of the system impulse response. This fundamental characteristic of shot noise allows it to be included easily in optical communication theory by adding together the variances of several Gaussian noise contributions. However, there is one more fundamental characteristic of shot noise that differentiates it from thermal noise. The power σ^2_{shot} of the shot noise generated during the photodetection process is *proportional* to the incident optical power level. In other words, the shot noise is intimately related to the average flux μ_{p} of detected particles, as it coincides with the fluctuations of the particle flux. This means that the shot noise generated during the photodetection process increases with received signal power. It is no longer a simple additive contribution, as in the case of thermal noise. We will see later the important consequences of this behavior.

1.2.3 Quadratic Term: Beat Noise

There are other contributions of noise involved in optical communications that have a *quadratic dependence* on the average optical power level P_{R} detected at the receiver input. In the following, we will consider briefly the case of the *signal-spontaneous beat noise* $\underline{n}_{\text{s-sp}}(t)$ generated by the coherent beating of the amplified optical signal and the amplified spontaneous emission noise in optical amplifiers [2, 3] operating at relatively high data rates. We will present an overview of the theory of beat noise in Chapter 2.

The optical amplifier provides amplification of the light intensity injected at the input by means of the *stimulated emission* process. In principle, every signal photon injected at the input section of the optical amplifier starts a multiplication chain while traveling along the active medium. At the output section of the optical amplifier, the input photon has been subjected to the average multiplication gain G, thus providing the corresponding light intensity average amplification. *The stimulated emission is a coherent process*: the generated (output) photon has the same energy

$$E = h\nu = \hbar\omega = \frac{hc}{\lambda} \tag{1.6}$$

and the same momentum

$$\mathbf{p} = \frac{E}{c}\mathbf{k} = \frac{h}{\lambda}\mathbf{k} \tag{1.7}$$

of the stimulating (input) photon. This is the most important property of the stimulated emission process: all generated photons, by means of the stimulated emission, have exactly the same energy and the same momentum of the injected photon. Note that the momentum is a vector quantity, as reported in Equation (1.7), specifying the direction of propagation of the photons. Since the energy of photons is proportional to the frequency of the electromagnetic field and the momentum of the photons is proportional to the direction of propagation **k**, we conclude that the stimulated emission provides a coherent amplification mechanism of the light intensity. This is the fundamental physical phenomenon inside every laser device ('laser' stands for Light Amplification by Stimulated Emission of Radiation).

In addition to stimulated emission, the quantum theory of interaction between light and matter predicts two other processes, namely *photon absorption* and *photon spontaneous emission*. Photon absorption and spontaneous emission are instead random processes, in the sense that we cannot predict exactly the instant of time at which the photon is either absorbed or spontaneously generated. The reason for this is that neither process is driven directly by the input signal field. However, every spontaneously emitted photon undergoes the same coherent amplification mechanism as every other signal photon. From this point of view, signal photons and spontaneously emitted photons are indistinguishable. Nevertheless, stimulated emitted photons and spontaneously emitted photons are not coherent; they have different energies (wavelengths) and different propagation directions. In general, optical amplifiers do not have any momentum-selective device installed, such as mirrors in the laser cavity. The spontaneous photons differ from the signal amplified photons in their broad energy spectrum and momentum. The spectrum of spontaneous emission is usually broad and coincides approximately with the optical amplifier bandwidth.

The spontaneous emission process is not correlated with the signal and behaves like a disturbing mechanism, degrading the intelligibility of the amplified signal. According to previous concepts, we easily identify *spontaneous emission as a noise phenomenon*, impairing the signal integrity of the optical amplification process. Owing to the optical amplification mechanism, we define this random process as *Amplified Spontaneous Emission (ASE) noise.* The beating process is not inherent to the optical amplifier itself; it is not part of the physics of the optical amplification. Instead, *beating noise is generated within the square-law photodetection process applied to the total electric field intensity available at the output of the optical amplifier*. Assuming that the optical field incident on the photodetector area is first filtered with an ideal optical filter of bandwidth $B_o > B_n$, the noise power of the photocurrent generated by the beating process between the signal and the ASE is proportional to the electrical bandwidth B_n and depends on the square of the received average optical power at the photodetector input. This means equivalently that the RMS amplitude of the signal-spontaneous beat noise current is proportional to the received average optical power level.

Sometimes the reader might misunderstand the quadratic dependence of beat noise on received optical power. The reason for this concern is that the received optical power must be carefully specified either at the optical amplifier input P_s or at the photodetector input P_R. However, these two power levels are related by the amplifier gain G, with $P_R = G(P_s)P_s$. In order to model the gain-saturation behavior of the optical amplifier, we have assumed that the gain G shows a functional dependence on the input optical power level P_s. Assuming low-signal input conditions, the amplifier gain is approximately independent of the input optical power, and the signal-spontaneous beat noise power increases approximately as the *square of the amplifier gain G*. For a fixed input optical power P_s, the signal-to-noise ratio at the

photodetector output exhibits a saturated behavior at relatively high levels of received optical power P_R. However, assuming a fixed optical amplifier gain, the signal-spontaneous beat noise power increases *linearly* with optical amplifier input power P_s, leading to the same mathematical model of signal shot noise as that introduced briefly above.

We deduce that, at relatively high levels of the received optical power P_R, the signal-spontaneous beat noise completely dominates the total noise composition in every optically amplified transmission systems, leading to the saturated *Optical Signal-to-Noise Ratio (OSNR)* and to corresponding performance limitation. Following the notation we specified previously, we indicate the power of the signal-spontaneous beat noise with the symbol $\sigma^2_{\text{s-sp}}$.

1.3 Total Noise

An important conclusion we should draw from these brief introductory concepts is that in optical communications there are *three* different noise functional dependences on the received average optical power level. We have identified the *constant term* (i.e. the thermal noise), the *linear term* (i.e. the signal shot noise), and the *quadratic term* (i.e. the signal-spontaneous beat noise). A peculiarity of the optical transmission system is the linear relationship between the received optical power and the photocurrent generated in the photodetector. This is the consequence of the square-law photodetection process, converting the optical intensity (*photon rate*, *number of detected photons per unit time*, proportional to the square of the incident electric field) into current intensity (*electron rate, number of generated electrons per unit time)*. After the photodetection process, the electrical signal amplitude (current or voltage) is then proportional to the received optical power.

As we have briefly touched upon in previous sections, the contributing noise terms might have different functional relationships with the received average optical power. It is a fundamental result of the theory of stochastic processes that the power of the sum of *stationary and independent* random processes is given by the sum of the power of each additive term. Assuming zero mean noise processes, the average power of the total noise is given by the following expression:

$$\sigma^2 = \sum_k \sigma_k^2 = \sigma^2_{\text{therm}} + \sigma^2_{\text{shot}} + \sigma^2_{\text{s-sp}} + \cdots \tag{1.8}$$

In particular, the functional dependence of the *RMS amplitude* σ of the total noise versus the received optical power, assuming statistically independent contributions, will present the constant term, the square-root term, and the linear term dependence:

$$\sigma = \sqrt{\sum_k \sigma_k^2} = \sqrt{\sigma^2_{\text{therm}} + \sigma^2_{\text{shot}} + \sigma^2_{\text{s-sp}} + \cdots} \tag{1.9}$$

The role of these three functional contributions is fundamental in understanding the noise limitations affecting optical transmission system performance. Figure 1.1 presents a qualitative drawing of the functional dependence of the three noise terms we have briefly examined. The intent is to give a clear picture of the diverse role of these noise components and to understand the way they lead to different sensitivity relationships.

At a very low level of received optical power, $P_R \ll P_a$ in Figure 1.1, the total noise is dominated by the *constant thermal noise* and other *signal-independent contributions.*

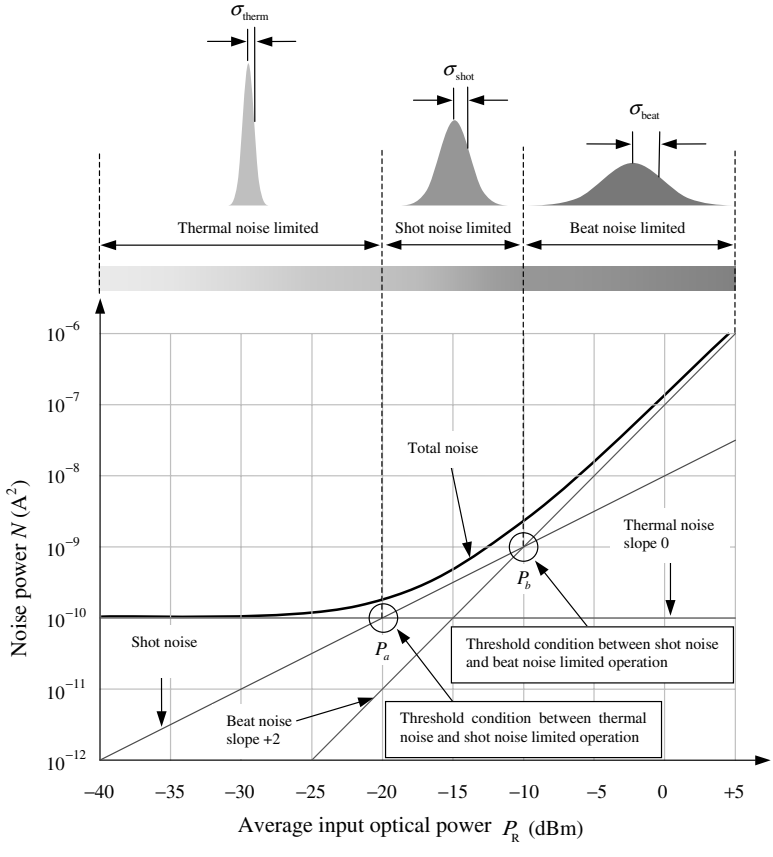

Figure 1.1 Qualitative representation of the three functional dependences of the noise contributions versus the average input optical power in optical fiber transmission systems. At relatively low optical power levels, the dominant noise term comes from the constant term as thermal noise. In fact, in the low power range, signal-dependent contributions are almost negligible, and the total noise remains almost constant. Increasing the optical power, the shot noise contribution becomes comparable with that of the thermal noise and the total noise power increases versus the optical power with a unit slope of 1 dec/10 dB. Increasing the optical power further makes the beat noise the dominant term in the total noise composition. The noise power slope reaches asymptotically twice the value exhibited in the shot noise limited range, with 2 dec/10 dB. The top line shows qualitatively the corresponding Gaussian approximate probability density functions of the stationary noise process

These noise terms act as *background noise*, limiting the minimum optical power that can be detected with the performance required:

$$\sigma \cong \sigma_{\text{therm}}, \quad P_{\text{R}} \ll P_a \tag{1.10}$$

Increasing the optical power, the *linear* signal-dependent noise contributions start growing relative to the background noise value, becoming the dominant contributor above the power threshold P_a. This is the optical power range usually dominated by the signal shot noise:

$$\sigma \cong \sigma_{\text{shot}} \propto \sqrt{P_{\text{R}}}\,, \quad P_a \ll P_{\text{R}} \ll P_b \tag{1.11}$$

Assuming no quadratic noise terms, in this interval the signal-to-noise RMS ratio improves as *the square root of the optical power*. In conclusion, under signal shot noise limited operation, the system performance can still be improved by increasing the optical power level incident at the receiver input, but at a lower rate than under constant noise conditions. In fact, the net improvement must account for the increasing signal shot noise too. At the circuit electrical decision section, the signal shot noise RMS amplitude increases by one-half of the slope of the signal amplitude, leading to a global performance improvement.

The situation is quite different if we introduce the third functional dependence considered above, namely the *quadratic* noise term, as illustrated by the signal-spontaneous beat noise contribution in an optically amplified transmission system.

In the following, suppose that the received optical power level P_{R} is increased by increasing the amplifier gain, with a fixed power P_{S} at the optical amplifier input. Assuming that the optical filter bandwidth is larger than the electrical noise bandwidth, the signal-spontaneous beat noise power has the following expression:

$$\sigma^2_{\text{s-sp}} = \frac{4q^2\lambda}{hc} n_{\text{sp}} G(G-1) B_n P_{\text{S}} \tag{1.12}$$

Substituting $P_{\text{R}} = GP_{\text{S}}$, we have

$$\sigma^2_{\text{s-sp}}(P_{\text{R}}) \cong \frac{4q^2\lambda}{hc} n_{\text{sp}} B_n \frac{P^2_{\text{R}}}{P_{\text{S}}}, \quad G \gg 1 \tag{1.13}$$

At a relatively higher power level, usually above the signal shot noise range, $P_{\text{R}} \gg P_b$ in Figure 1.1, and the RMS beat noise amplitude increases linearly with the photocurrent signal amplitude, leading to a saturated signal-to-noise RMS ratio with limited system performance:

$$\sigma \cong \sigma_{\text{s-sp}} \propto P_{\text{R}}, \quad P_{\text{R}} \gg P_b \tag{1.14}$$

From this point on, any further optical power increase does not have any benefit, determining the proportional RMS beat noise increment. This is the typical operating condition of every DWDM optical transmission system using optical amplifiers at the receiver end. In this case, transmission system performance is mainly determined by the signal-spontaneous beat noise, demanding that the sensitivity requirements specified for the optical amplifier parameter specifications be specified instead for the PIN-based optical receiver.

A second relevant example of the quadratic noise term is the *Relative Intensity Noise (RIN)* in laser sources [4]. The RIN is defined as the ratio between the power spectral density $S_{\underline{I}}(f)$ (dBm/Hz) of the detected photocurrent process $\underline{I}_{\text{R}}(t)$ and the squared value $\langle \underline{I}_{\text{R}}(t) \rangle^2$ of the average photocurrent $I_{\text{R}} \equiv \langle \underline{I}_R(t) \rangle = RP_{\text{R}}$. The constant quantity R is the photodetector responsivity and depends linearly on the product of the wavelength λ and the conversion efficiency $\eta(\lambda)$. According to the definition, the RMS noise amplitude of the RIN contribution depends linearly on the received average optical power, setting a limiting condition on the maximum achievable signal-to-noise ratio:

$$\sigma_{\text{RIN}}(P_{\text{R}}) = RP_{\text{R}} \sqrt{B_n \text{RIN}} \tag{1.15}$$

where we have introduced the noise bandwidth approximation applied to the uniform power spectral density $S_{\underline{I}}(f)$ (dBm/Hz) of the relative intensity noise process.

1.4 Bit Error Rate Performance

In this book we will focus on the *Intensity Modulation Direct Detection (IMDD)* optical communication system. This is the basic and most widely used optical transmission technique for both short-reach and high-density distribution networks and ultralong-reach backbone optical links. In spite of the simplicity of the baseband optical transmission technique, millions of kilometers of installed single-mode and multimode fibers have been networking the whole world for more than 20 years. The success of this simple transmission format relies both on the extremely large modulation bandwidth exhibited by the optical fiber and on the high-speed intensity modulation and detection capabilities of semiconductor-based laser sources and photodetectors.

It is well known that the success of optical communication is founded on the coincidence between the optical transmission windows of low-cost silica-based optical fibers and the emitted spectrum of the direct band-gap compound semiconductor light sources. Of course, after initial pioneering experiments in the late 1970s using GaAs semiconductor lasers emitting at 850 nm and silicon detectors, man-made optical communication technology took giant strides towards improving performance consistency, working towards optical transmission window optimization, developing a far more complex semiconductor laser structure, and designing exotic refractive index profile fibers for almost dispersionless transmission and state-of-the-art band-gap engineered photodetectors for almost ideal light capture, with astonishing results.

It is a strange peculiarity of optical fiber communication that, instead of withdrawing more complex but quite efficient modulation formats from radio and wireless engineering in the past 20 years, using existing technology with appropriate developments, optical fiber communication engineering has been focused, from the very beginning, on the most dramatic and far-reaching technology improvements while still relying on the crudest transmission principle ever conceived, namely the *Intensity Modulation Direct Detection (IMDD)* technique. Recently, owing to the continual push towards higher transmission rates over longer distances, some different modulation formats have been considered, but, again, the optical technology is making greater strides, supplying new ideas and using unexpected physical phenomena in order to present alternative solutions to more consolidated light modulation formats. Fiber nonlinearities, for example, have been attracting great interest over a period of at least 10 years because of the undiscovered capabilities of optical soliton transmission in reaching extremely long distances at terabit capacity.

As already mentioned, in this book we will consider the many noise impairments concerning the basic IMDD transmission system. The choice of the IMDD transmission technique is, of course, fundamental in developing an appropriate theory of system performance degradation in the presence of all the noise components affecting the optical signal. The most commonly used technique for evaluating the performance of optical fiber transmission is based on the *bit error rate (BER)*. Assuming IMDD transmission, the received optical field intensity is detected and converted into the corresponding photocurrent. The noise affecting the signal comes from different sources, as briefly touched upon above. We will address *noise source partitioning* in the next part of this introduction.

The information bit is represented by the photocurrent sampled at the decision instant and is affected by all noise contributions. The acquired sample then represents the sum of the true signal embedded and several noise terms. The amplitude binary decision is the simplest process conceivable in recognizing each one of the two logical states available. Binary direct detection is sometimes referred to as *On-Off Keying (OOK)*, and by analogy with the conventional digital modulation formats as *Amplitude-Shift Keying (ASK)*, *Frequency-Shift Keying (FSK)*, *Phase-Shift Keying (PSK)*, and so on. The decision rule reduces therefore to recognizing when the sampled amplitude is above or below the logic threshold level. In optical communication this decision process reduces to recognizing the light or the dark conditions associated with the detected signal at the sampling instant. Of course, we associate logic state *1* with light recognition and logic state *0* with the absence of light (dark). Even if it seems quite obvious, we should point out that we are dealing with the photodetected current pulses associated with corresponding optical fields. Intersymbol interference, timing jitter, and noise components, either additive or signal related, all contribute to obscuring the original signal content of the detected sample, leading to erroneous identification of a light sample instead of a dark one, and vice versa. This erroneous bit recognition leads directly to error generation in the decision procedure.

The BER is the process of counting the erroneously detected bits in relation to the total number of detected bits. It corresponds to the relative frequency of erroneous bit detection and for very large numbers it coincides with the error probability P_e of the decision process.

What is the Origin of Error Generation in IMDD Optical Transmission Systems?
As mentioned above, the decision process in IMDD optical transmission systems is a very basic and crude process, limited to the recognition only of the *threshold crossing condition* of the decision circuit. In the following, we will use $\underline{s}_k = \underline{s}(t_k)$ to denote the random variable representing the general photocurrent sample picked up at sampling instant t_k. The best way to analyze the problem is ideally to separate the signal sample $\underline{s}_k = \underline{s}(t_k)$ into the sum of two distinct quantities: the ideal *deterministic pulse sample* $\underline{b}_k$, represented as a discrete random variable assuming one of two possible values $\underline{b}_k = \{b_0, b_1\}$, and the *amplitude perturbing random variable* $\underline{r}_k = \underline{r}(t_k)$, including all the remaining disturbing effects:

$$\underline{s}_k = \underline{b}_k + \underline{r}_k \tag{1.16}$$

Figure 1.2 shows a qualitative picture of the binary amplitude decision model we are discussing. We can now answer the question formulated above: each error originates when the amplitude perturbing random variable $\underline{r}_k = \underline{r}(t_k)$ presents a *finite probability* to cross the decision threshold, leading to erroneous recognition of the complementary logic state.

It should be clear from these introductive concepts that the error generation does not depend exclusively on the amount of noise sampled at the decision instant t_k but is strongly influenced by the intersymbol interference and the timing jitter which add further fluctuations to the decision process. These concepts will be formulated precisely in the following chapters of this book.

The graphical representation in Figure 1.2 shows the probability density functions of the random variables $\underline{b}_k = \{b_0, b_1\}$ and $\underline{r}_k = \underline{r}(t_k)$, corresponding respectively to the signal and to the noise samples captured at the ideal decision instant t_k. As will be shown in some detail in Chapter 2, the bit error rate for the Gaussian noise distribution is represented by the

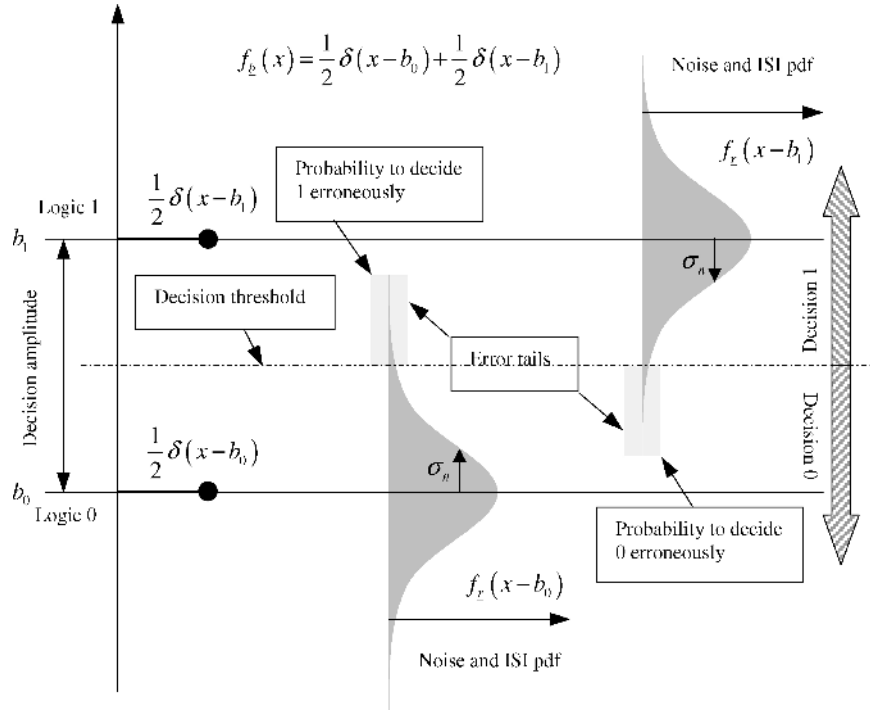

Figure 1.2 Graphical representation of the amplitude decision process for a binary signal embedded with noise. In this model we have assumed that the signal amplitude adopts each discrete value with the same probability (1/2). The probability density function (pdf) of the random process identified by the sum of the signal and the noise is given by the convolution of the respective probability density functions. In this case, the convolution reduces simply to translating the noise pdf over the respective signal amplitudes. The error condition is represented by the amount of noise pdf crossing the threshold level (light gray boxes)

complementary error function, whose argument, the Q-factor, is defined by the ratio between the decision amplitude $b_1 - b_0$ and twice the total RMS noise value σ:

$$Q \triangleq \frac{b_1 - b_0}{2\sigma}$$
$$Q_{\mathrm{dB}} \triangleq 20\log_{10} Q \tag{1.17}$$

and

$$\mathrm{BER} = \frac{1}{2}\mathrm{erfc}\frac{Q}{\sqrt{2}} \tag{1.18}$$

Figure 1.3 gives a qualitative representation of the Q_{dB}-factor in Equation (1.17) and the corresponding bit error rate curves given by Equation (1.18) versus the received average optical power, assuming the three different functional dependences of noise contributions that have been briefly introduced above. As the RMS noise amplitude of the sum of statistically independent processes adds quadratically, it is possible to identify the single component of the Q-factor for each noise contribution by defining

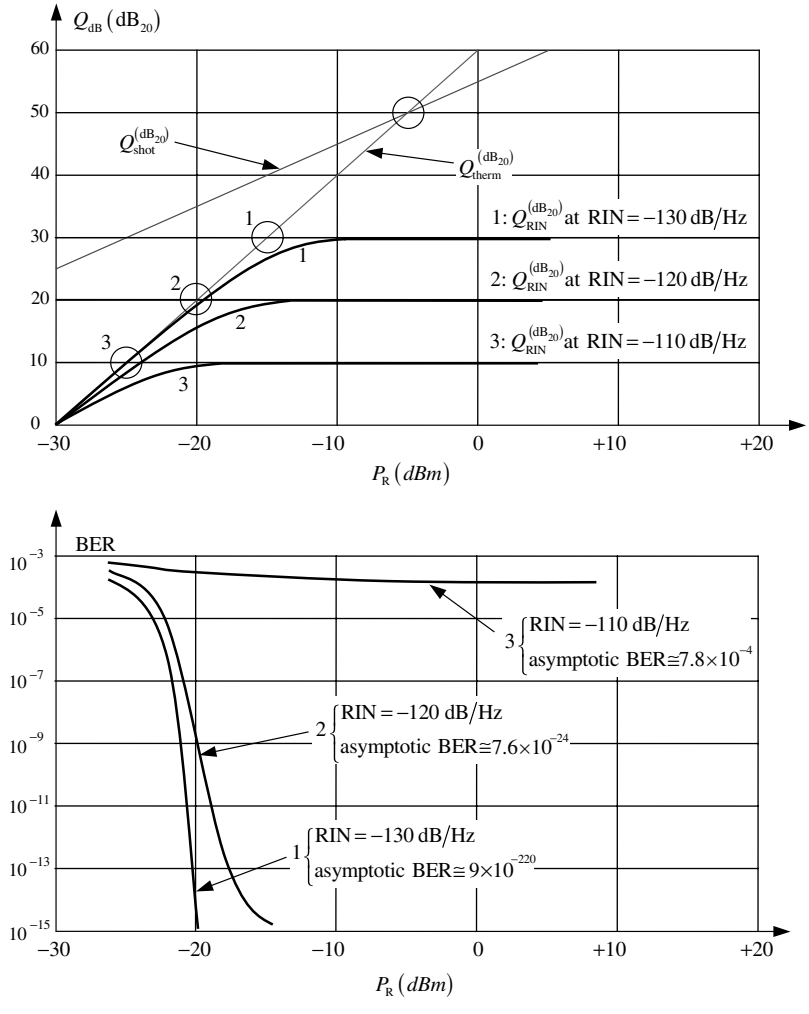

Figure 1.3 Qualitative drawing of the Q-factor and the BER function versus the receiver average optical power, assuming the parameter set of Equations (1.25). The dependence on the quadratic noise term is responsible for the flooring behavior of the BER performance

$$Q_k \triangleq \frac{b_1 - b_0}{2\sigma_k} \tag{1.19}$$

The Q-factor relative to the total noise, from Equations (1.8), (1.17), and (1.18), becomes

$$\frac{1}{Q^2} = \sum_k \frac{1}{Q_k^2} = \frac{4}{(b_1 - b_0)^2} \sum_k \sigma_k^2 = \frac{4\sigma^2}{(b_1 - b_0)^2} \tag{1.20}$$

At relatively low optical power levels, the dominant *thermal noise* leads to the steepest Q-factor and BER slopes. In the thermal noise limited condition, the Q_{dB}-factor in

Equation (1.19) gains 20 dB every decade of increment in the received optical power. In the higher power range, the effect of shot noise becomes comparable with that of constant thermal noise, leading to an appreciable reduction in the slopes of the Q-factor and in the corresponding BER performance. In the shot noise limited condition, the Q_{dB}-factor in Equation (1.19) gains one-half of the thermal noise case, increasing only 10 dB every decade of increment in the received optical power. Finally, in the highest power range, the quadratic dependence of the beat noise contribution leads to saturated profiles of both the Q-factor and the BER, exhibiting well-known BER floor behavior. Above this range, any further increment in received optical power does not result in any error improvements, and the performance of the transmission system cannot be improved any further.

In the following, we will report expressions for the partial contribution to the Q-factor of the three functional noise dependences considered so far, namely the constant thermal noise, the linear signal shot noise, and the quadratic RIN term. These expressions will be carefully derived later in this book. For the moment, we will use them in order to have a quantitative comparison among several noise terms. Assuming an infinite extinction ratio and an equiprobable NRZ symbol sequence, the *Optical Modulation Amplitude (OMA)* coincides with twice the average optical power P_{R} and the decision amplitude $b_1 - b_0 = 2RP_{\mathrm{R}}$. Substituting into Equation (1.19), we have

$$Q_k = \frac{RP_{\mathrm{R}}}{\sigma_k} \tag{1.21}$$

For the three specific noise components mentioned above, we have the following expressions:

$$Q_{\mathrm{therm}}^{(\mathrm{dB}_{20})} = 10\log_{10}\left[\frac{R^2}{B_n\langle i_c^2\rangle}\right] + 2P_{\mathrm{R}}^{(\mathrm{dBm})} - 60 \tag{1.22}$$

$$Q_{\mathrm{shot}}^{(\mathrm{dB}_{20})} = 10\log_{10}\left(\frac{R}{2qB_n}\right) + P_{\mathrm{R}}^{(\mathrm{dBm})} - 30 \tag{1.23}$$

$$Q_{\mathrm{RIN}}^{(\mathrm{dB}_{20})} = -10\log_{10}B_n - \mathrm{RIN} \tag{1.24}$$

where $\langle i_{\mathrm{c}}^2\rangle$ is the power spectral density of the input equivalent noise current from the electric receiver (A^2/Hz), R is the responsivity of the photodetector (A/W), B_n is the noise bandwidth (Hz), and RIN is the relative intensity noise coefficient (dB/Hz).

It is clear from the above expressions that the functional dependence versus the average input optical power of the Q-factor relative to the thermal noise has twice the slope of the Q-factor corresponding to the shot noise limited conditions. The Q-factor relative to the RIN term is constant, as expected. Note that the expression for the Q-factor is given by Equation (1.20), and that the individual contributions (Equations (1.22), (1.23), and (1.24)) assume the dominant role only under noise limited conditions. The following parameter values refer to the application range for the 10 Gb/s optical fiber transmission system operating according to the ITU-T STM-64 or to the equivalent Bellcore-Telcordia GR-253-CORE OC-192 specification. The numbers reported below are intended only as an indication of the considered calculation:

$$\begin{aligned} R &= 1\,\mathrm{A/W} \\ B_n &= 10\,\mathrm{GHz} \\ i_{\mathrm{c,rms}} &= 10\,\mathrm{pA}/\sqrt{\mathrm{Hz}} \\ \mathrm{RIN} &= \left\{ \begin{array}{c} -130 \\ -120 \\ -110 \end{array} \right\} \mathrm{dB/Hz} \end{aligned} \tag{1.25}$$

Substituting these values into Equations (1.22), (1.23), and (1.24), we have the following linear relationships in log-log scale representation:

$$Q_{\mathrm{therm}}^{(\mathrm{dB}_{20})} = 60 + 2P_{\mathrm{R}}^{(\mathrm{dBm})}\ \mathrm{dB} \tag{1.26}$$

$$Q_{\mathrm{shot}}^{(\mathrm{dB}_{20})} \cong 55 + P_{\mathrm{R}}^{(\mathrm{dBm})}\ \mathrm{dB} \tag{1.27}$$

$$Q_{\mathrm{RIN}}^{(\mathrm{dB}_{20})} = \left\{ \begin{array}{c} 30 \\ 20 \\ 10 \end{array} \right\} \mathrm{dB} \tag{1.28}$$

We can see that, at the optical power value $P_{\mathrm{R}}^{(\mathrm{dBm})} = -5$ dBm, the individual Q-factors of the thermal noise and the signal shot noise are equal. We have assumed three different values of RIN in order to see the relevance of the quadratic noise effect on the saturated performance. In the example considered we see that the lower RIN value, RIN $= -130$ dB/Hz, does not add any significant contribution to the total Q-factor and hence does not change the corresponding BER performance. From Figure 1.3 we see that the computed asymptotic BER value reaches the unpractical small value of $\approx 10^{-219}$! In this case, even if the total Q-factor is determined by the combination of all noise contributions, we conclude easily that the thermal noise sets the BER performance while the RIN and the signal shot noise are completely negligible. Increasing the RIN value by 10 dB, up to RIN $= -120$ dB/Hz, raises the asymptotic BER to $\approx 10^{-23}$. Again, this limitation does not interfere with the usual transmission system BER specification set at $\approx 10^{-12}$.

However, owing to the high slope of the error function, increasing the RIN coefficient slightly leads to disastrous degradation of the system error performance. This is demonstrated well in the third case considered. In fact, assuming that RIN $= -110$ dB/Hz, we obtain the unacceptable asymptotic BER of $\approx 10^{-3}$, more than 20 dec higher than in the previous case. In order to finalize our qualitative understanding of the relationship between noise contributions and BER curves, Figure 1.4 shows computed results for the same case as that discussed so far. The plots have been generated using source code written in MATLAB® (MATLAB® is a registered trademark of The MathWorks Inc.) R2008a (The MathWorks, Inc., Natick, MA). The Q-factor and the BER have been computed using expressions (1.18), (1.20), (1.22), (1.23), and (1.24) with the data reported in Equations (1.25), without any approximation.

The computed BER performance clearly shows the predicted flooring behavior associated with higher quadratic noise contributions. For moderate RIN coefficients in the range $-130\,\mathrm{dB/Hz} \leq \mathrm{RIN} \leq -120\,\mathrm{dB/Hz}$, the BER plots follow closely the profile determined by the dominant thermal noise contribution and exhibit almost the same high negative slope versus the received average optical power.

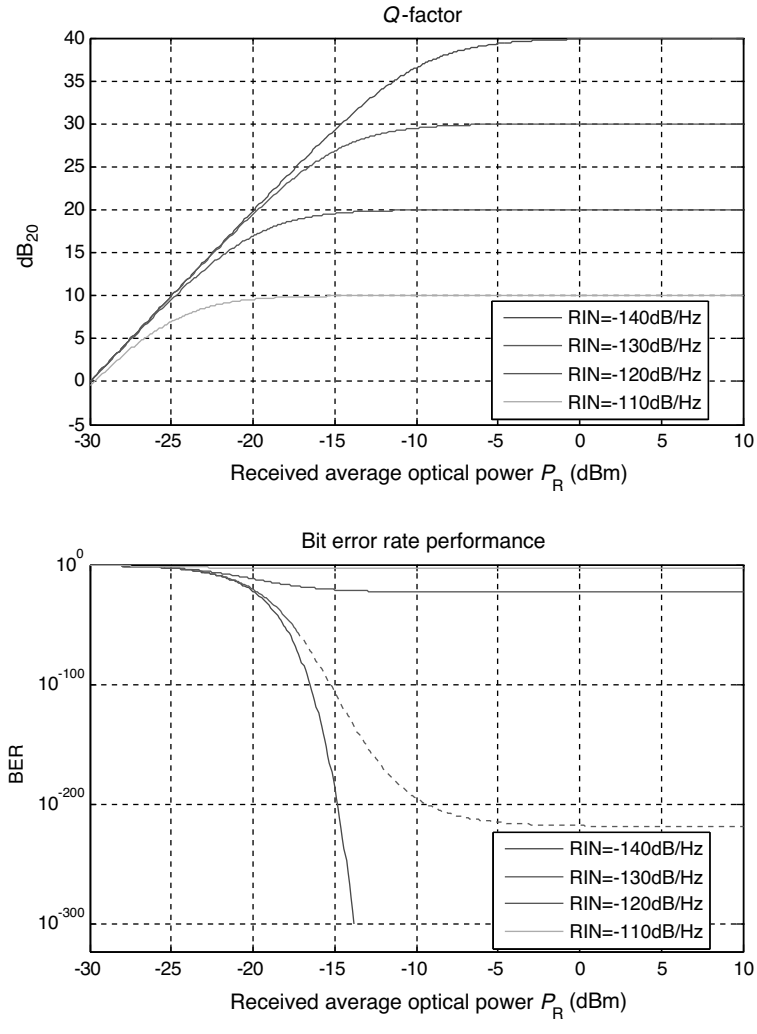

Figure 1.4 Computed plots of the Q-factor (upper graph) and the corresponding bit error rate (lower graph) for the case considered in the text, using full-scale representation. The flooring behavior of the BER curves on account of the quadratic noise term is evident at higher values of the laser relative intensity noise

This behavior is clearly shown in Figure 1.5, where the reduced error range $10^{-16} \leq \text{BER} \leq 10^{-1}$ used on the vertical scale highlights the thermal noise limited operation. However, at higher RIN coefficients, the strong quadratic noise contribution becomes predominant and hardly limits the BER close to 10^{-3}, making the transmission system performance unacceptable, unless sophisticated *Forward Error Correcting (FEC)* code techniques are implemented.

Before concluding this introduction concerning noise contributions and error probability, it would be instructive to consider one more aspect of the consequences of quadratic noise terms.

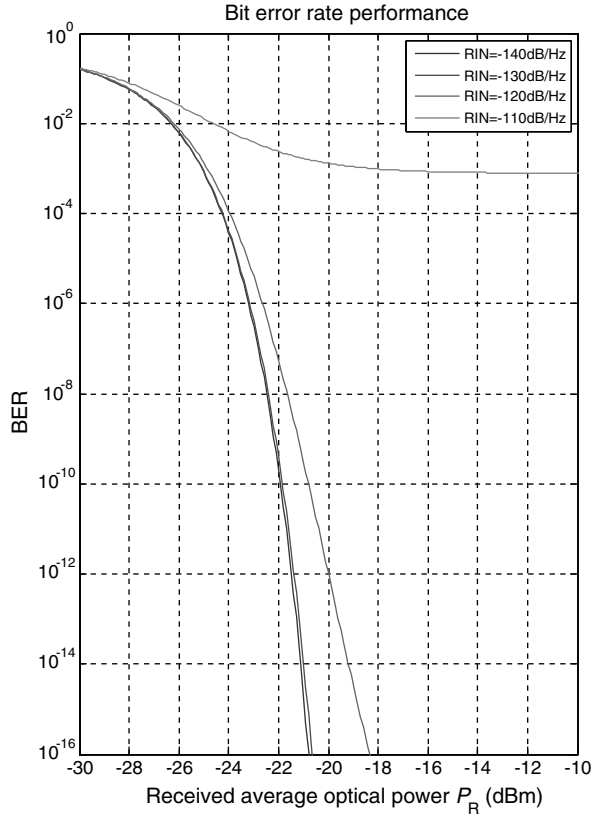

Figure 1.5 BER plots for the same case as Figure 1.4 but represented in a reduced error scale for practical purposes. The typical BER range of interest for telecommunications is $10^{-3} \leq \text{BER} \leq 10^{-13}$. Strong flooring behavior of the BER, which is associated with RIN $= -110$ dB/Hz, limits the minimum error rate close to 10^{-3}

From Figure 1.5 it is clear that limiting the error rate to BER $\leq 10^{-12}$, as is usually required by standard telecom specifications, and setting RIN ≤ -120 dB/Hz, any flooring behavior is observed in the computed BER curve. Nevertheless, if the RIN is close to -120 dB/Hz, an appreciable *optical power penalty* is observed. This is a significant effect of the quadratic tail contribution, even several decades above the saturated floor profile. Figure 1.6 shows details of the computed BER in a limited power range. Referring to the BER plot associated with RIN $= -120$ dB/Hz, we observe an optical power penalty of about 2 dB evaluated at a reference error rate of 10^{-12}. The displacement is the effect of the quadratic noise contribution over the thermal noise. In conclusion, quadratic noise terms affect the BER plots even several decades above the error probability asymptote, leading to consistent degradation of transmission system performance. The same considerations hold for the linear noise terms, with minor consequences for the quadratic noise terms.

In order to take a step forward in generalizing the bit error rate analysis, we should include the effect of timing jitter in the previous discussion. The theory of jitter impairments will not be

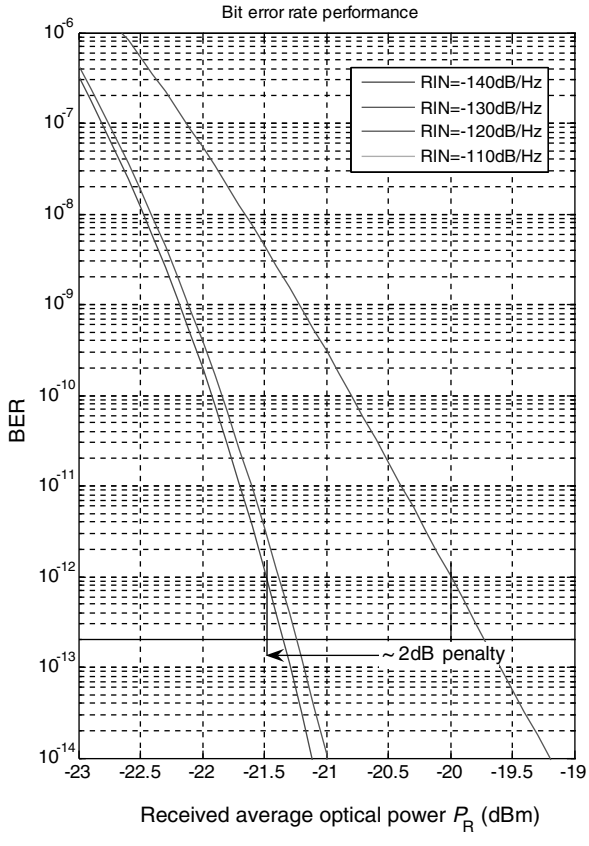

Figure 1.6 Representation of the computed bit error rate in a reduced range of the average received optical power. The effect of the quadratic noise contribution can be clearly seen as a displacement from the thermal noise limit. In the case considered, the optical power penalty is measured at an error rate of 10^{-12} between the two BER plots associated respectively with RIN $= -140$ dB/Hz and RIN $= -120$ dB/Hz. The degradation, assuming RIN $= -130$ dB/Hz, is almost negligible

discussed further in this book, but some concepts and considerations regarding the timing jitter effect will be reported below.

1.5 Timing Jitter

Signal recognition in digital transmission systems is based on the synchronous acquisition of the information bit by sampling the received signal at a fixed clock rate. The clock signal is usually extracted by the incoming signal spectrum by means of the *Clock and Data Recovery (CDR)* circuit. Figure 1.7 presents a schematic block diagram of the CDR topology with *Phase Locked Loop (PLL)*-based clock extraction.

The incoming data stream is usually divided into two branches, one of which is used to extract the clock frequency, and the other for data recovery and the retiming operation. The

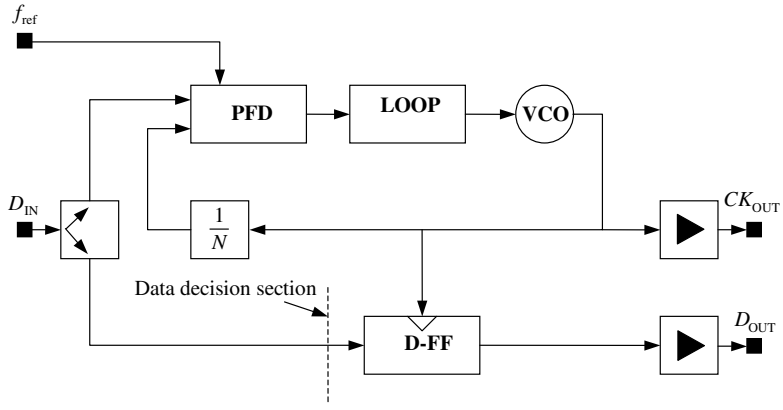

Figure 1.7 Block diagram of the active CDR topology using the PLL technique. The data input signal is used by the *Phase Frequency Detector (PFD)* to lock the internal *Voltage Controlled Oscillator (VCO)* on the appropriate data phase in order to provide optimum data retiming and regeneration at the *D-Flip-Flop (D-FF)* output. The VCO frequency is divided for simplified PFD operation and low-frequency reference clock signals. Two output buffers provide additional driving capabilities and other signal features

clock frequency can be extracted by means of either passive or active solutions. However, referring to the most used NRZ transmission format, we will note that the signal spectrum does not include any line at the corresponding data rate frequency, and the CDR must provide some nonlinear mechanism to generate the required clock frequency. This feature must be present in every CDR, regardless of whether it adopts passive or active extraction architecture. Passive extraction is accomplished using very narrow-bandwidth filters implemented with either *Dielectric Resonator (DR)* or *Surface Acoustic Wave (SAW)* technology.

Active clock frequency extraction is based on PLL architecture with the internal *Voltage Controlled Oscillator (VCO).*

As an example, Figure 1.8 reports the maximum permissible jitter specification at the OTU2 interface for STM-64 (10 Gb/s) optical transmission systems, according to the ITU-T G.otnjit

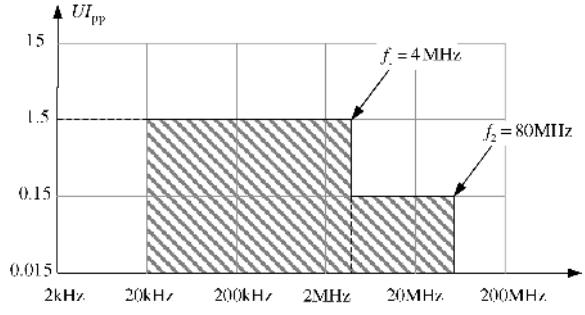

Figure 1.8 ITU-T G.otnjit mask specification for maximum permissible jitter at the OTU2 interface operating at the 10 Gb/s standard data rate. The peak-to-peak jitter is referred to as the *Unit Interval (UI)*

standard [5]. The specification gives the maximum allowed peak-to-peak jitter, expressed in terms of the *Unit Interval (UI)*. The UI coincides with the bit time step for the selected transmission rate. In the case of the OTU2 interface for STM-64, the data bit rate is $B = 9953.280$ Mb/s.

Owing to the application of *Forward Error Correcting (FEC)* code for improving transmission performance, the *symbol line rate* is increased according to the ratio 255/237, leading to the increased line bit rate $B_{\text{line}} = 10\,709.23$ MB/s. The corresponding unit interval for the line bit rate therefore assumes the value UI = 93.38 ps. The ITU-T G.otnjit specification requires that the peak-to-peak jitter in the frequency interval $4\,\text{MHz} \leq f \leq 80\,\text{MHz}$ be lower than $0.15\text{UI} \cong 14$ ps. Figure 1.9 shows a qualitative drawing of the data signal eye diagram at the decision section (see Figure 1.7) with principal parameter definition. It is important to point out that the signal performance must be evaluated *prior* to the decision process.

Decision errors, phase skew, jitter, and noise are all impairments that are effective *only before* the signal sample has been decided.

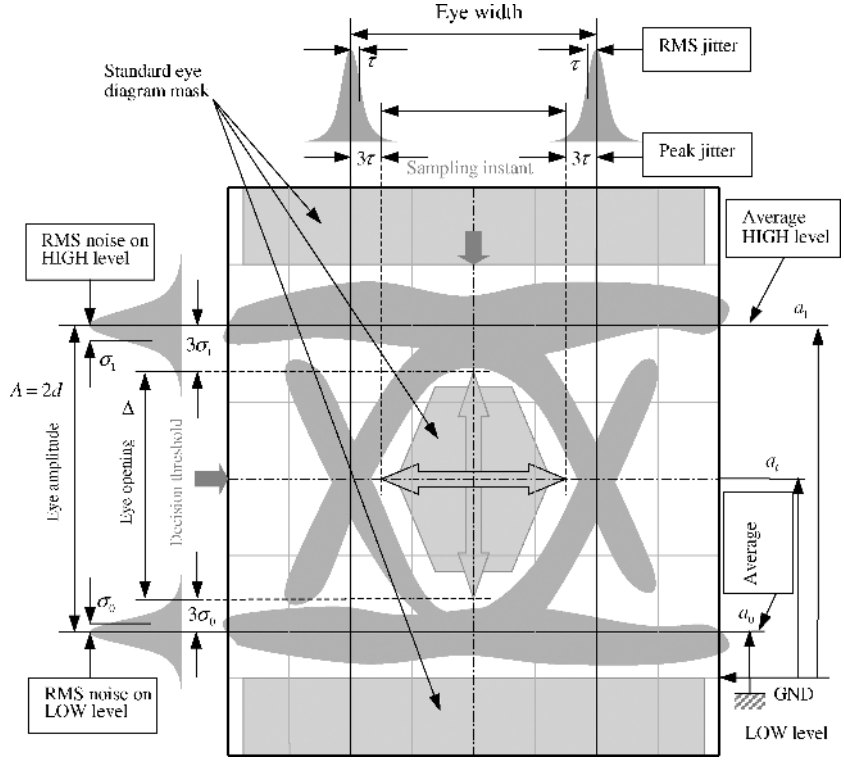

Figure 1.9 Schematic representation of the eye diagram at the decision section, assuming NRZ binary transmission format. The principal parameters are shown as they appear in standard laboratory measurement equipment. The two logic levels are referred to the common ground potential (GND), but the error rate performance is related only to relative quantities, the eye opening and the eye width respectively. In this representation, peak quantities are defined as 3 times the corresponding RMS values

How Does Jitter Affect the Amplitude Decision Process?

We will come back to this question later on, to show the full derivation of the decision model under simultaneous amplitude noise and jittered time conditions. In spite of the general theory, we believe it would be worthwhile in this general introduction to give hints as to the way in which amplitude noise and timing jitter interact to determine erroneous binary decision conditions. This will serve as an introduction to the general treatment that will be followed in the coming chapters. To this end, we will consider the signal pulse at the decision section to be referred to a stable, fixed timeframe, affected only by constant-amplitude noise distributed with a Gaussian probability density function of fixed RMS width σ over both signal levels. The decision instant, referred to the same timeframe as above, is a random process whose fluctuations are described by means of temporal jitter with a Gaussian probability density function of fixed RMS width τ. These conditions can be qualitatively referred to the eye diagram shown in Figure 1.9 above. The gray-shaded area represents qualitatively the uncertainty region for the signal crossing under noise and jitter conditions.

The problem can be correctly approached using the concepts of the conditional probability and the related total probability theorem. Recall that the conditional probability of event $\mathcal{A}$, assuming the conditioning event $\mathcal{B}$, is defined by the following ratio:

$$P(\mathcal{A}|\mathcal{B}) = \frac{P(\mathcal{A}\mathcal{B})}{P(\mathcal{B})} \tag{1.29}$$

If $\mathcal{M} = [\mathcal{B}_1, \ldots, \mathcal{B}_N]$ is a partition of the whole event space $\mathcal{S}$

$$\begin{aligned} &\bigcup_{k=1}^{N} \mathcal{B}_k = \mathcal{S} \\ &\mathcal{B}_j \cap \mathcal{B}_k = \varnothing, \quad j,k = 1,2,\ldots N,\ j \neq k \end{aligned} \tag{1.30}$$

the probability of the arbitrary event $\mathcal{A} \subset \mathcal{S}$ is given by

$$P(\mathcal{A}) = \sum_{k=1}^{N} P(\mathcal{A}|\mathcal{B}_k)P(\mathcal{B}_k) \tag{1.31}$$

This equation constitutes the total probability theorem. Figure 1.10 gives a qualitative representation of the partition of the event space.

Referring to the signal amplitude decision process, we can easily identify the jittered decision time as the conditioning event $\mathcal{B}$ and the corresponding symbol error as the conditioned event $\mathcal{A}|\mathcal{B}$. In the continuous event space with jittered decision time, the bit error rate coincides with the total probability of making an erroneous decision under the conditioning decision time process with the probability density function $\phi_{\underline{t}}(t)$:

$$\mathrm{BER} = \int_{-\infty}^{+\infty} P\{\text{Decision error}|\ \underline{t} = t\}\phi_{\underline{t}}(t)\mathrm{d}t \tag{1.32}$$

Of course, in the notation above, the probability of the event $\{\text{Decision error}|\ \underline{t} = t\}$coincides with the bit error rate evaluated at the decision instant $\underline{t} = t$.

Figure 1.11 gives a qualitative indication of the mathematical modeling of the amplitude decision process under the jittered time conditions just introduced. In particular, if the timing

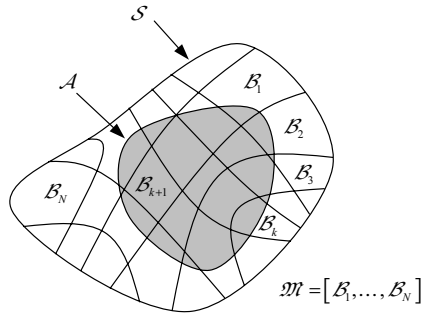

Figure 1.10 Event space representation using the partition $\mathcal{M} = [\mathcal{B}_1, \ldots, \mathcal{B}_N]$. The event $\mathcal{A} \subset \mathcal{S}$ is decomposed over the partition $\mathcal{M} = [\mathcal{B}_1, \ldots, \mathcal{B}_N]$, with the conditional probabilities $P(\mathcal{A}\mathcal{B}_k) = P(\mathcal{A}|\mathcal{B}_k)P(\mathcal{B}_k)$. The total probability of the event $\mathcal{A} \subset \mathcal{S}$ is given by the sum of the partial contributions $P(\mathcal{A}\mathcal{B}_k)$ over the entire space partition

process were ideal, with no jitter at all, sampling at the deterministic time instant $t = t_0$, the corresponding probability density function of the random variable $\underline{t}$ would collapse upon the delta function $\phi_{\underline{t}}(t) = \delta(t - t_0)$ and Equation (1.32) would reduce to the well-known expression $\text{BER}_{(t=t_0)} = P\{\text{Decision error}\}$. As we will see in Chapter 3, the *Power Spectrum Density (PSD)* of the stationary jitter random process, under some assumptions, can be approximated by the Lorenzian curve, and the first-order probability density function by a Gaussian distribution.

1.6 Partition of Noise Sources

In order to consider the different noise contributions affecting the optical detection and decision processes, we should specify first the architecture of optical fiber transmission systems and the modulation format used for symbol coding. As outlined briefly in previous sections, optical fiber transmission is affected by numerous noise sources, some attributable to the electrical domain, others peculiar to the optical solution adopted. In addition to noise source diversity, recall that components of the noise in optical systems have different functional relationships with the received optical power, setting different limitations on the transmission system performance. A clear example of this behavior is represented in Figure 1.12, which shows a comparison between system A, equipped with the bare PIN-based direct detection optical receiver, and system B, using instead the optically preamplified direct detection optical receiver.

The two receivers have the same structure, and we can assume that they use the same photodetector and even the same transimpedance amplifier. In other words, systems A and B in Figure 1.12 are considered to have the same optical receiver, but system B has in addition an optical preamplifier in front of the PIN receiver. At this point we are not concerned about optimizing the architecture of the two receivers but rather focus on the different roles of the noise terms involved in determining the optical receiver performances.

Referring to system A and assuming typical operating conditions, the sensitivity of the optical receiver is determined by the *thermal noise* generated by the electronics of the front-end transimpedance amplifier. Accordingly, we expect the BER to decrease with the fastest slope as the received optical power increases. Typically, at an error rate of 10^{-12} the decaying slope is more than 1 dec over a few tenths of a dB of increment in the received input optical power.

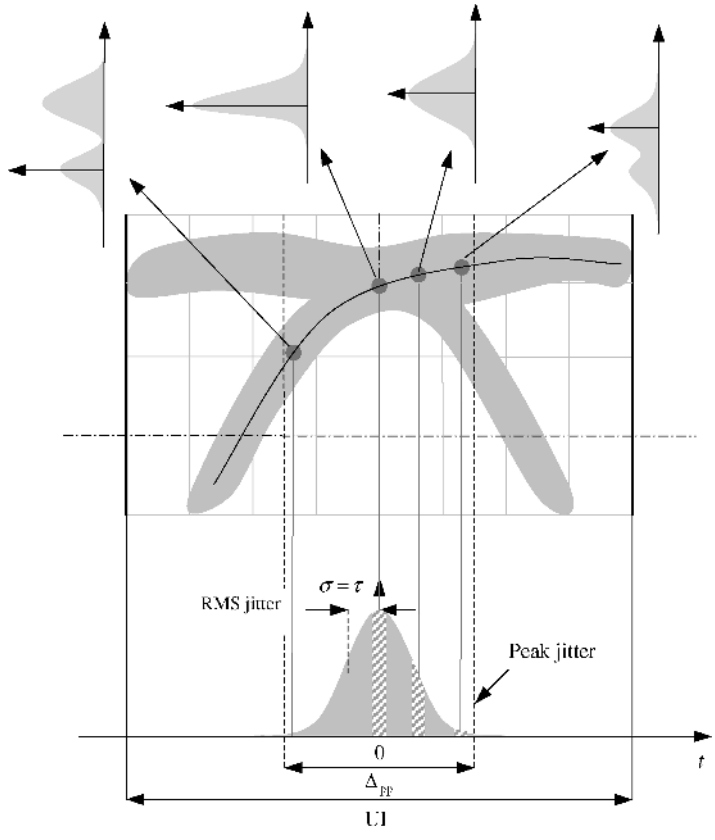

Figure 1.11 Graphical representation of the calculation of the total error probability of the amplitude decision process with noisy and jittered conditions. The jitter probability density function is represented in green and is assumed to be centered on the ideal sampling time. The timing fluctuations lead to a specific weight for each contribution to the total error probability. Once the conditional event of a particular sampling time is accounted for, the error probability contribution depends on the corresponding amplitude noise distribution at the local time, as is qualitatively shown in the figure for four different sampling time instants

Equivalently, we expect the Q-factor in Equation (1.17) to increase proportionally to the received average input optical power, showing a constant slope of 20 dB/dec. To enable a quantitative comparison between the systems considered, we will assume the following parameter set:

$$\begin{aligned} \lambda &= 1550\,\text{nm} \\ \eta &= 0.8 \\ B_n &= 10\,\text{GHz} \\ \langle i_c^2 \rangle &= 2 \times 10^{-22}\,\text{A}^2/\text{Hz} \\ n_{sp} &= 1.4 \\ G &= 0 - 30\,\text{dB} \end{aligned} \tag{1.33}$$

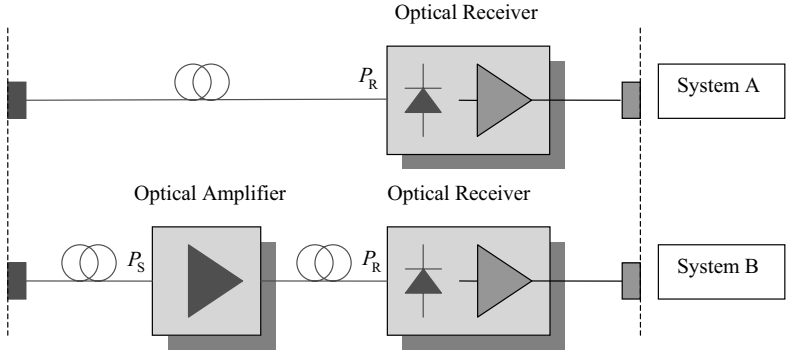

Figure 1.12 Block diagrams of the simple PIN-based optical receiver and the optically preamplified optical receiver. Solutions A and B are both assumed to deploy the same PIN diode and the same electronic receiver. The sensitivity of system A is limited by the signal-independent thermal noise of the electronics, while the sensitivity of system B is determined by the quadratic dependence of the signal-spontaneous beat noise of the optical preamplifier

The total noise power of system A is given by the thermal noise contribution only:

$$\sigma^2_{\text{therm}} = \langle i_c^2 \rangle B_n \cong 2 \times 10^{-12}\,\text{A}^2 \tag{1.34}$$

The performances of system A are plotted in Figure 1.13 for the case of amplifier unity gain, $G = 1$. In fact, from Equation (1.12) we can see that, for $G = 1$, the signal-spontaneous beat noise contribution is null and the total noise coincides with the thermal noise only. As expected, the computed Q-factor and BER plots pass through $Q \cong 17$ dB and BER $= 10^{-12}$ respectively at the received average optical power $P_R = -20$ dBm. This is consistent with the assumptions of the thermal noise power spectral density $\langle i_c^2 \rangle$ and noise bandwidth B_n in parameter set (1.33).

The plot of the Q-factor corresponding to amplifier unity gain clearly shows the expected slope of 20 dB/dec. This results in the steepest achievable BER plot in the lower graph in Figure 1.13.

The situation is completely different for system B operating with the optical amplifier. The total noise power is given by the sum of the contributions of the thermal noise and the signal-spontaneous beat noise. From expressions (1.34) and (1.12) we have

$$\sigma^2 = \left[\langle i_c^2 \rangle + \frac{4q^2\lambda}{hc} n_{sp} G(G-1) P_S \right] B_n \tag{1.35}$$

Figure 1.13 presents the computed performances versus the average optical power at the amplifier input for three different gain values. Recall that the case of unity gain coincides with the configuration of system A. At relatively low gain, $G = 10$, the effect of the beat noise is almost negligible at low power levels, $-40\,\text{dBm} \leq P_S \leq -30\,\text{dBm}$, and the computed plot of the Q-factor reports almost the same slope of system A, showing still dominant thermal noise operations. At increasing power levels, the beat noise starts to dominate the total noise and the slope of the Q-factor decreases accordingly, showing the expected asymptotic value of 10 dB/dec. At higher gains, the behavior is similar but the power ranges are shifted towards lower values. It is important to note that, owing to the quadratic noise contribution, higher gains

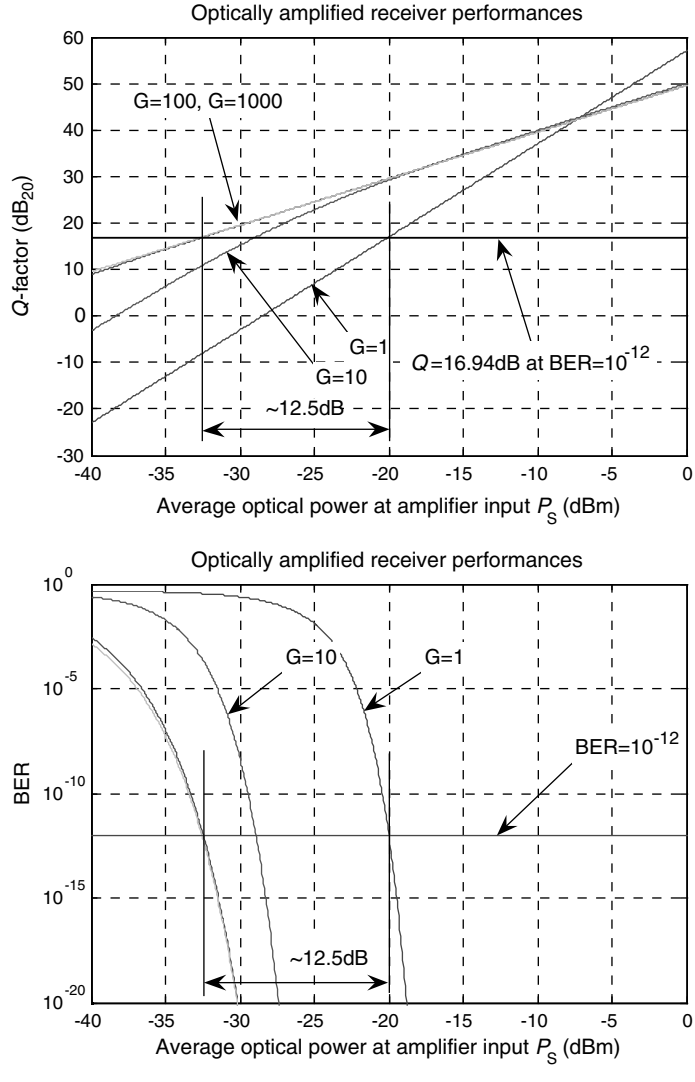

Figure 1.13 Computed performances of system A and system B for parameter set (1.33). The upper graph shows the Q-factor versus the average optical power available at the optical amplifier input. The horizontal solid line corresponds to the value of the Q-factor required for achieving a bit error rate of 10^{-12} under Gaussian noise conditions and equiprobable symbols. The plot corresponding to the amplifier unity gain refers to system A, and the slope of the Q-factor shows the expected constant value of 20 dB/dec. The performances of system B are reported for three different amplifier gain values $G = 10$, 100, and 1000. The corresponding plots of the Q-factor show the increasing effect of the signal-spontaneous beat noise at increasing optical power levels. The lower graph shows the computed BER values for the same cases as those in the upper graph

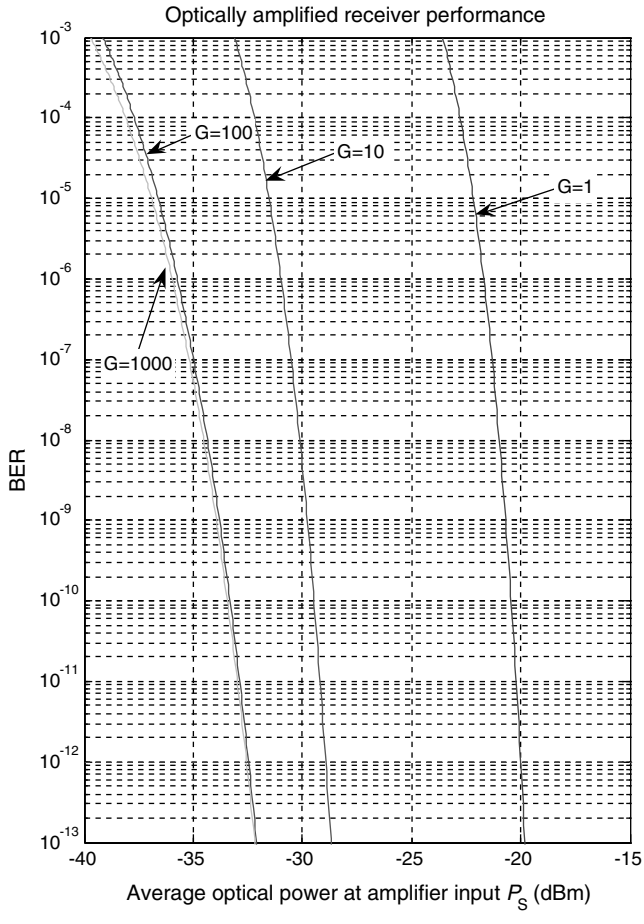

Figure 1.14 Computed BER performances for transmission system B with parameter set (1.33). The case $G = 1$ coincides with system A, without an optical amplifier. Increasing the amplifier gain leads to system sensitivity improvements with a reduced slope owing to the beat noise contribution. In this case, the amplifier gain benefit saturates at approximately $G = 100$, with about 12.5 dB sensitivity improvement over the value reported by reference system A

do not improve the performance of system B. This is clearly shown in Figure 1.13 by the negligible improvements between the cases of $G = 100$ and $G = 1000$.

An important conclusion emerging from these calculations is that, using the optical amplifier with a gain $G \approx 100$, system B shows a sensitivity improvement of about $\Delta P_S \cong 12.5$ dB in relation to system A. This clearly demonstrates the benefit of using the optical amplifier. However, we see that increasing the gain above $G \approx 100$ does not result in any improvement on account of spontaneous emission noise. These considerations should give clear directions for designing transmission systems with optical amplifiers. Usually a gain of 20 dB is enough to have transmission system performances limited by the amplifier beat noise

and not by the PIN receiver sensitivity. Of course, it follows that using high sensitivity and more sophisticated receivers equipped with an *Avalanche Photo Detector (APD)* would result only in a waste of money, leading to the same performance as that of the low-cost PIN-based receiver. Figure 1.14 reports the same plots as Figure 1.13 on a more suitable scale. At the

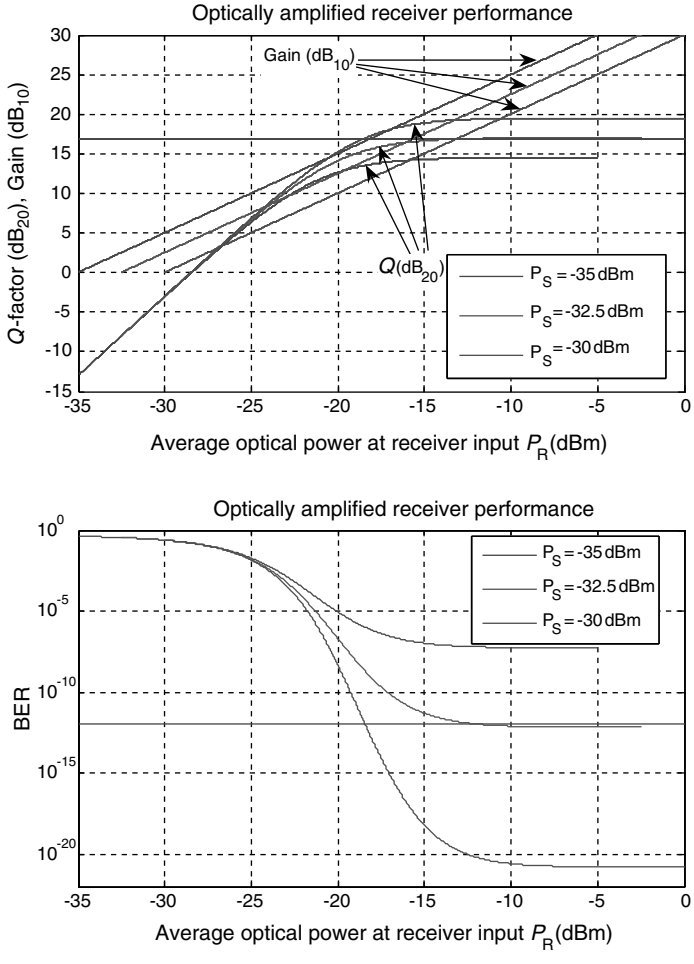

Figure 1.15 Computed performances of transmission system B versus the average optical power P_R at the receiver input, assuming parametric variation in the average optical power P_S at the optical amplifier input. The power P_R is varied by means of the amplifier gain G. The upper graph shows the Q-factor and the amplifier gain G versus P_R. It is clear in this example that system B reaches the minimum Q-factor required for the reference error rate BER $= 10^{-12}$ only in the case of $P_S = -30$ dBm. The corresponding optical power P_R is given by the intersection between the plot of the Q-factor and the horizontal line corresponding to the reference value $Q_{ref} \cong 17$ dB. The lower graph shows the BER plots that satisfy the corresponding reference value BER $= 10^{-12}$ at the same optical power level. The saturation behavior of the Q-factor (upper graph) for higher values of the received optical power and the corresponding BER floor (lower graph) are evident

reference BER $= 10^{-12}$, transmission system improvement versus amplifier gain is clearly demonstrated.

In order to gain more confidence with the optical amplifier operation, Figures 1.15 and 1.16 report the computed performances of the same systems A and B versus the average optical

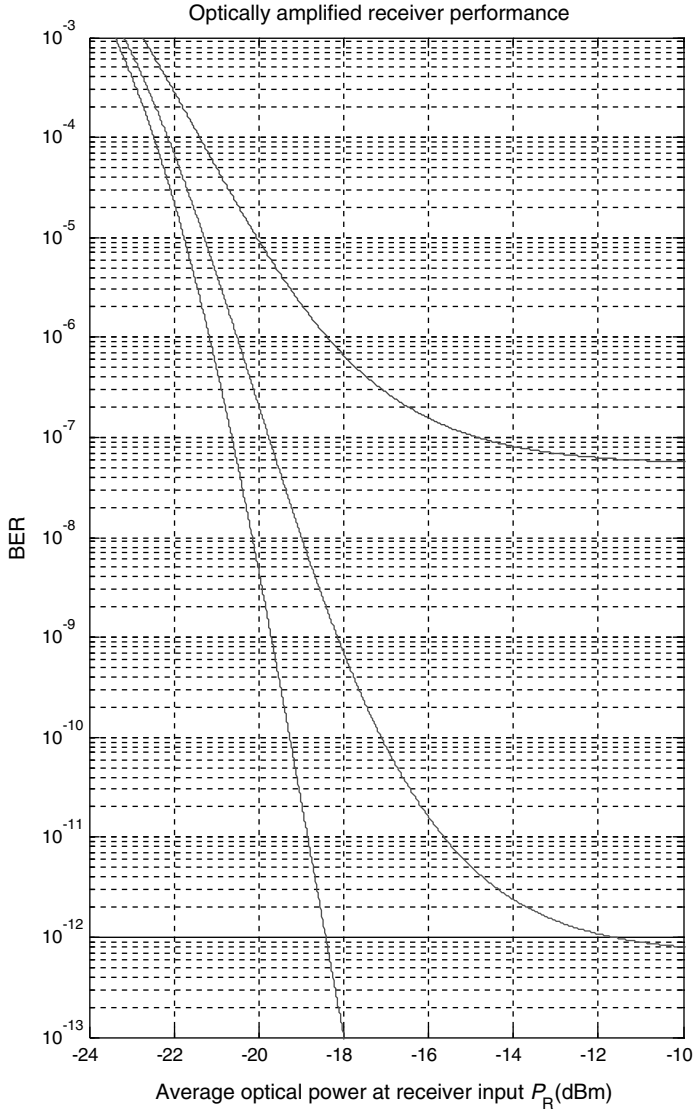

Figure 1.16 Computed error rate performances for system B operating under the same condition as Figure 1.15. The lower value of the vertical scale has been limited to 10^{-13} in order to allow better plot resolution. The BER flooring corresponding to lower values of the average optical power at the amplifier input is evident. In these cases, in fact, the higher gain required increases the signal-spontaneous beat noise, leading to a dominant quadratic noise contribution

power P_R evaluated at the PIN-based receiver input, instead of the average power P_S at the optical amplifier input. Figure 1.16 shows a detailed view of the error rate plots in the region of interest.

Figure 1.17 presents a detailed view of the Q-factor and amplifier gain versus the average input optical power P_R, assuming a fixed amplifier input power $P_S = -30$ dBm. The circle in the

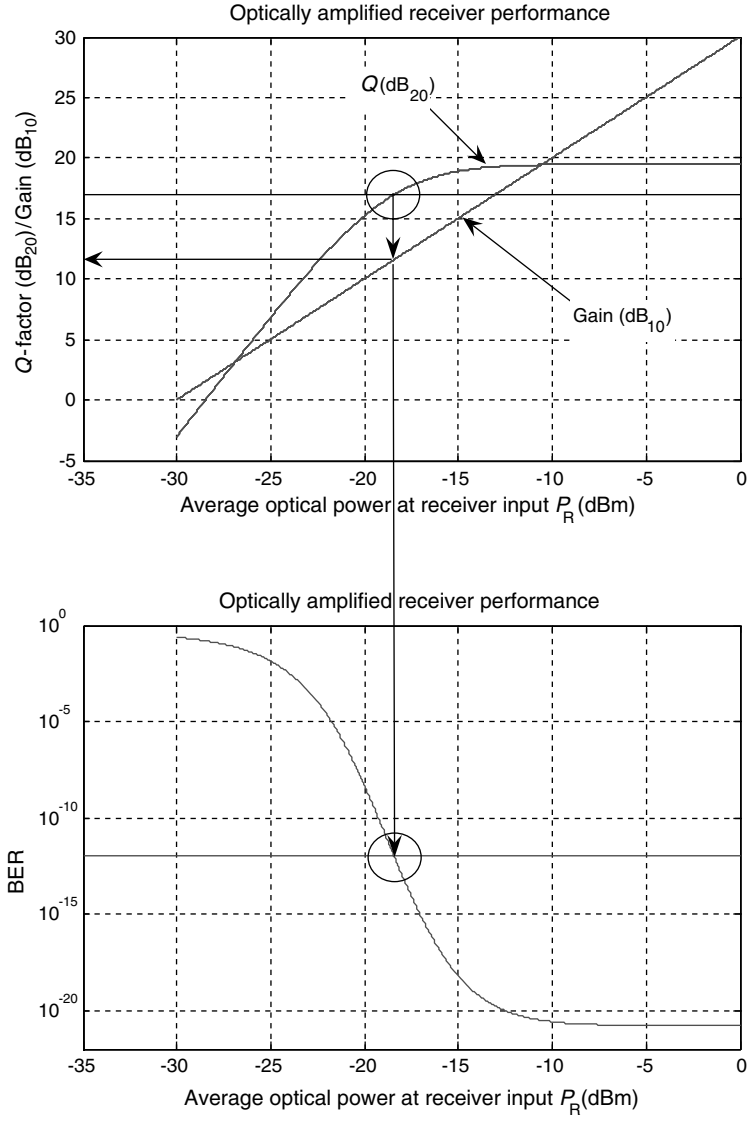

Figure 1.17 Graphical calculation of the amplifier gain and average optical power at the receiver input for achieving the required Q-factor, $Q_{\text{ref}} \cong 17$ dB and error rate BER $= 10^{-12}$. Higher values of the amplifier gain are associated with lower error rates, but the signal-spontaneous beat noise leads to saturation behavior of the system performance

upper graph highlights the intersection region for the required Q-factor. The corresponding amplifier gain is easily found by reading the corresponding value on the left scale. In the case considered, we find approximately $G \cong 12\,\text{dB}$ and $P_R \cong -18\,\text{dBm}$. The same value of the received optical power in the lower graph leads to the required BER $\cong 10^{-12}$.

1.7 Conclusions

In this chapter we have introduced several aspects of the amplitude and phase noise contributing to the degradation of optical fiber transmission performance. To show these effects, we used the three most typical noise functional relationships versus received average optical power, namely the thermal noise (constant), the signal shot noise (linear), and the signal-spontaneous beat noise (quadratic). We discussed their effect on the bit error rate performance for the direct detection intensity modulated optical system, introducing important engineering concepts such as the slope of the error rate and, in particular, the existence of asymptotic limiting behavior, known as the BER floor. The BER floor is achievable only if a dominant quadratic noise term occurs in the error detection process. We introduced the concept of partitioning of noise sources, referring to the different transmission system contexts in which some noise contributions become relevant, in spite of others not appearing at all.

System design usually encounters only a few relevant noise terms, depending on the source and receiver technologies, the fiber link specification, and the transmission architectures. However, optical communication system designers must be well aware that, behind new technological choices usually adopted for improving signal transmission, system capacity, and other market-oriented features, different noise contributions can impact severely on the desired system characteristics, leading to unexpected overall performance degradation. The correct starting point in making choices for system improvement is a profound knowledge of the noise-related outcome.

References

[1] Papoulis, A., '*Probability, Random Variables and Stochastic Processes*', 3rd edition, McGraw-Hill, New York, NY, 1991.

[2] Desurvire, E., '*Erbium Doped Fiber Amplifiers – Principles and Applications*', Wiley Interscience, New York, NY, 1994.

[3] Olsson, N.A., 'Lightwave Systems with Optical Amplifiers', *IEEE Journal of Lightwave Technology*, **7**, July 1989.

[4] Petermann, K. and Weidel, E., 'Semiconductor Laser Noise in an Interferometric System', *IEEE Journal of Quantum Electronics*, **17**, July 1982.

[5] ITU-T G.otnjit, '*The Control of Jitter and Wander within the Optical Transport Network*', March 2001.